Statics Correction Methods For 3D Converted-Wave (PS) Seismic Reflection

Shaun Strong*†and Steve Hearn*†

December 20, 2016

ABSTRACT

One of the most difficult steps in the PS processing sequence is estimation of the S-wave receiver statics. This process is particularly important at the coal scale, due to the need for higher frequency content (better resolution).

We present an analysis of three approaches for estimating 3D PS statics. These include a surface-consistent inversion algorithm (analogous to the residual-statics method used in conventional P-wave processing), PPS refraction statics, and a so-called robust statistical method. This analysis is achieved through the use of synthetic models, and a coal-scale 3D-3C survey acquired in the Bowen Basin.

The presented datasets demonstrate that the surface-consistent inversion method can become unstable in certain environments. This is likely due to parameter leakage between receiver and structural terms, caused by the highly asymmetric nature of the shallow PS reflection paths. The robust statistical method appears reliable for determination of short-wavelength receiver statics, and hence is useful for continuity enhancement. The PPS refraction approach can provide both short-wavelength and long-wavelength solutions, provided the PPS arrivals can be picked reliably. As with P-wave analysis, a combination of algorithms may provide the most effective production tool for determination of PS receiver statics.

* Velseis Pty Ltd, Brisbane, Australia
† School of Earth Sciences, University of Queensland, Brisbane, Australia.

INTRODUCTION

The converted-wave (PS) seismic reflection method has been used for hydrocarbon exploration since the mid 1980s (Stewart *et al.,* 2002). The technique has mainly been used for 2D surveys but it has also had limited use in 3D exploration (e.g. Simin *et al.,* 1996; Brzostowski *et al.,* 1999). PS-wave reflection has proven most valuable in situations where conventional P-wave methods have encountered problems, such as imaging structures in the presence of gas (eg. MacLeod *et al.,* 1999). One of the reasons why PS reflection has not been more generally applied is that PS processing is relatively complex and time consuming. A particularly difficult step in the PS processing sequence is determination of S-wave receiver statics.

Statics are time delays caused by variations in the near surface. These time errors cause misalignment between traces which are to be combined in the stacking process. This introduces smearing, and hence loss of continuity and resolution on the stacked images.

In the case of land surveys acquired with surface sources, static errors arise mainly from weathering-related time delays in the vicinity of the source and receiver. In PS reflection, a P-wave source is used. Hence the source static can be derived from the conventional P-wave data, normally acquired in conjunction with the PS survey. The receiver static arises when the reflected S-wave passes through the weathering layer. The S-wave velocity at the surface tends to be considerably lower, and more variable, than the P-wave velocity. This tends to result in relatively large and variable S-wave receiver statics and increases the complexity of statics estimation.

For shallow high-resolution surveys the problem of static errors is further emphasised, since correction of these is more important when imaging smaller targets. In 2D-PS coal surveys, statics have consistently been found to have a significant effect on the quality and resolution of seismic sections (e.g. Hearn *et al.,* 2003; Hendrick *et al.,* 2007).

It has been pointed out (e.g. Hearn *et al.,* 2003) that PS-wave data could, in theory, be used to image small structures with greater resolution. This is due to the lower velocity, and hence potentially shorter wavelength, of the S-wave. In practice, for resolution of PS reflection events to be better than conventional P-wave reflection events, the frequency content on the stacked sections need to be comparable. Unfortunately, in many cases the frequency content is much less for PS data (e.g. Hearn, 2004). One factor that may

contribute to this is incorrect estimation of the weathering statics (Strong & Hearn, 2008).

For PS data the S-wave receiver statics have traditionally been calculated using three different approaches. These consist of those based on analysis of horizon timing differences on common-receiver-gathers (CRG); refraction methods including PPS and SSS waves; and scaled P-wave statics (e.g. Vargas *et al.,* 2011). More recent areas of study also include a technique based on correlation of adjacent CRGs (Guevara *et al.,* 2015); ray-path interferometry via the radial trace or Tau-p domains (e.g. Henley, 2014; Cova *et al.,* 2015); and inversion of surface-wave dispersion data (e.g. Socco *et al.,* 2015; Yang *et al.,* 2012).

In this investigation three different PS statics algorithms have been examined with the intention of improving the image quality of an example 3D seismic volume. The methods used are surface-consistent PS-wave statics, a method we refer to as the robust statistical method, and PPS refraction analysis. In the following, each method is outlined and the advantages are examined via 2D numerical models and a real 3D dataset.

OUTLINE OF METHODS

Surface-Consistent PS-Wave Statics

The standard method of calculating the receiver statics in our coal-scale 2D-PS work is based on the P-wave residual statics approach. In the conventional P-wave residual technique reflection horizons are usually automatically picked on CMP gathers via correlation methods. Each time error (δt) is assumed to be a linear function of time values associated with the source (δt_s), receiver (δt_r), structure (δt_{cdp}) and residual NMO (δt_{off}).

$$\delta t \approx \delta t_s + \delta t_r + \delta t_{cdp} + \delta t_{off} \tag{1}$$

Based on this model, the error on each trace can be attributed to individual parameters in a surface-consistent manner, using a least-squares inversion algorithm.

For PS data, the conventional technique is difficult to implement since CCP binning requires a good understanding of velocities. However, PS velocities are more difficult to determine due to a lower signal-to-noise ratio and

larger statics. Therefore, a modified residual statics method has been developed (Hendrick *et al.,* 2007).

Selected PS-reflection horizons are manually picked in the receiver domain. For the 2D case, limited-offset receiver-domain stacks are picked. This allows the general RMS velocity to be calculated as a parameter of the inversion and removes the need for the application of an accurate NMO solution before statics calculation.

PS processing is usually conducted in conjunction with the conventional P-wave analysis. Hence, the P-wave source static correction can be applied to the PS data before the S-wave receiver-statics calculation. Therefore, the remaining PS static error (δt) can be parameterised into receiver (δt_r), structural (δt_{ccp}), and offset (δt_{off}) contributions.

$$\delta t \approx \delta t_r + \delta t_{ccp} + \delta t_{off} \tag{2}$$

In 2D-PS surveying it is common to separate the positive and negative offsets and process these separately (Thomsen, 1999). Sometimes this includes calculating separate statics solutions. For the 3D case this corresponds to grouping traces according to the source-to-receiver azimuth direction. That is, the reflection horizons are picked on limited-offset and limited-azimuth receiver stacks. Therefore, by modifying equation 2 to include an azimuthal term ($\delta t_{azimuth}$) we can investigate the degree of azimuthal variability in receiver statics. The modified equation used in the azimuthal least-squares inversion is given by

$$\delta t \approx \delta t_r + \delta t_{ccp} + \delta t_{off} + \delta t_{azimuth} \tag{3}$$

PPS Refraction Statics

A standard method for calculating conventional P-wave statics is to analyse refraction events. For P-wave data this requires the picking of the high-energy first-arrivals, which generally correspond to the PPP refraction events. Differences in these picks can be analysed to derive the source and receiver statics (e.g. Lawton, 1989). For PS data the corresponding concept is to pick the PPS refraction (Hearn & Meulenbroek, 2011; Meulenbroek & Hearn, 2011). This event is generated by conversion of the critically refracting P wave to an upward travelling S headwave (Figure 1). Since the S wave is slower than the P wave, the PPS refraction may not be the first

arrival. In addition, the strength of the PPS refraction can be quite variable. These factors often make the PPS event difficult to identify.

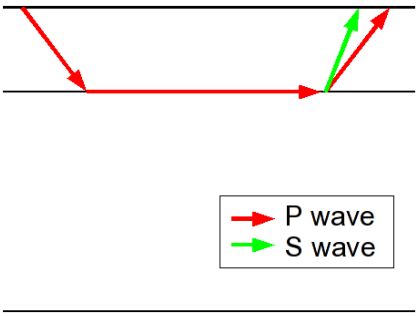

Figure 1: Conventional (PPP) and converted (PPS) refraction raypaths.

For shallow 2D-PS surveys this technique may be difficult to apply, since there are often not enough picks to give an accurate solution. This is especially true for surface sources where surface waves tend to swamp much of the PPS refraction energy. For high-fold 3D surveys even if the PPS event can only be picked for a small percentage of the total number of traces there may still be enough to derive a viable statics solution.

For this investigation we have used the time-term method to extract the receiver statics (Reiter, 1970; Ralston, 2015). The technique assumes that the time of each refraction pick is a function of a source term (t_s), a receiver term (t_r), and an offset term (t_{off}).

$$t = t_s + t_r + t_{off} \tag{4}$$

To allow for lateral variations in the refractor, we have expressed the offset term (t_{off}) as the summation of time elements over all bins traversed by the refracting wave (Figure 2).

$$t_{off} = \sum_k \frac{d_k}{v_k} \tag{5}$$

The source term (t_s), the receiver term (t_r), and the bin velocities (v_k) are the unknowns. The observed times for all available rays provide an overdetermined set of equations. We have used Singular Value Decomposition to estimate the unknown parameters in a least-squares sense.

Solving these equations without constraints tends to give some anomalous velocities which create errors in the receiver responses. The results have

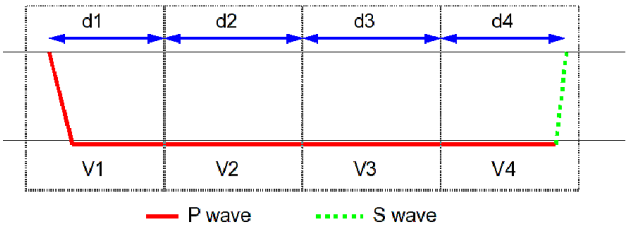

Figure 2: Graphical representation of a time-term ray path showing decomposition into offset bins.

been improved by constraining anomalous velocities to the average velocity. An interesting numerical consideration relates to instability resulting from scale differences between the unknown times and unknown velocities. This can cause cross contamination between parameters. The robustness of the inversion is generally improved by expressing unknown velocities in km/s (and distances consequently in km). This ensures that variations of the unknowns are on the same order of magnitude.

The time terms t_s and t_r are equivalent to time depths (or delay times) at source and receiver (e.g. Hearn & Meulenbroek, 2011). The receiver term relates to weathering depth (Z) and weathering S-wave velocity (v_{1S}) via

$$t_r = \frac{Z \cos i_{1S}}{v_{1S}} \tag{6}$$

where i_{1S} is the angle made by the upcoming PPS head wave. This angle is small because of the large contrast between the S-wave velocities of the weathering layer and the P-wave velocities of the subweathering. Hence the receiver time term is approximately equal to the S-wave travel time through the weathering, and can be treated as a weathering static.

Robust Statistical Statics

During this investigation we have also developed a technique that utilises robust statistical algorithms to calculate the receiver statics solution. This so-called robust statics method (outlined in Figure 3) is related to the method proposed by Cary & Eaton (1993), although it differs in the handling of reflector structures. This implementation uses the same offset-limited receiver-domain horizon-picks that are selected for the surface-consistent-statics approach (e.g. Figure 3a). This allows the robust statistical method to be investigated in parallel with the surface-consistent approach for very little extra effort.

It is important to remember that the horizon picks are a function of the static at the receiver, the offset, the structure and possible azimuthal variations (equation 3). The zero-Hz component of the horizon-picks, corresponding to the offset component, is removed for each limited-offset panel (e.g. Figure 3b). From this the long-wavelength components, consisting of long-wavelength structural and receiver terms, are removed using smoothers (e.g. Figure 3c). The remaining short-wavelength components are combined using robust statistical methods such as median filters and averaging (e.g. Figure 3d). A key assumption of this process is that it cancels out the short-wavelength structural terms and returns the short-wavelength receiver statics. This tends to be true if the fold of the data is high, and if we err on the side of caution when choosing our smoothing operators. This technique also assumes that the short-wavelength receiver statics are not azimuthally varying, which is reasonable for low-velocity weathering layers where the ray-paths are near vertical.

Since the long-wavelength component contains both structural and receiver terms, which cannot be separated, the main aim of this approach is to improve the stack quality. The consequence of this is that it may not give a correct structural image. However, this shortcoming can be overcome by incorporating long-wavelength statics from an alternative algorithm, or by tying the stacked reflection events to borehole data.

2D VISCOELASTIC MODELLING

To gain a better understanding of the advantages and limitations of each of the statics calculation techniques we have applied visco-elastic finite-difference modelling to a typical coal-scale model (Figure 4). This allows vertical and inline shot records to be produced which are processed using standard production algorithms. The modelling does not easily produce static shifts so a statics profile has been designed (Figure 5) and applied via a surface-consistent approach. Only the receiver statics have been added. Following the approach taken with real data, it is assumed that the conventional P-wave source corrections have already been applied.

Figure 6 shows an example of an offset-limited receiver stack from the modelled data. The horizon picks corresponding to the upper reflector are also included. For this investigation various offset ranges have been examined. However, we have focused on the mid offsets as there tends to be

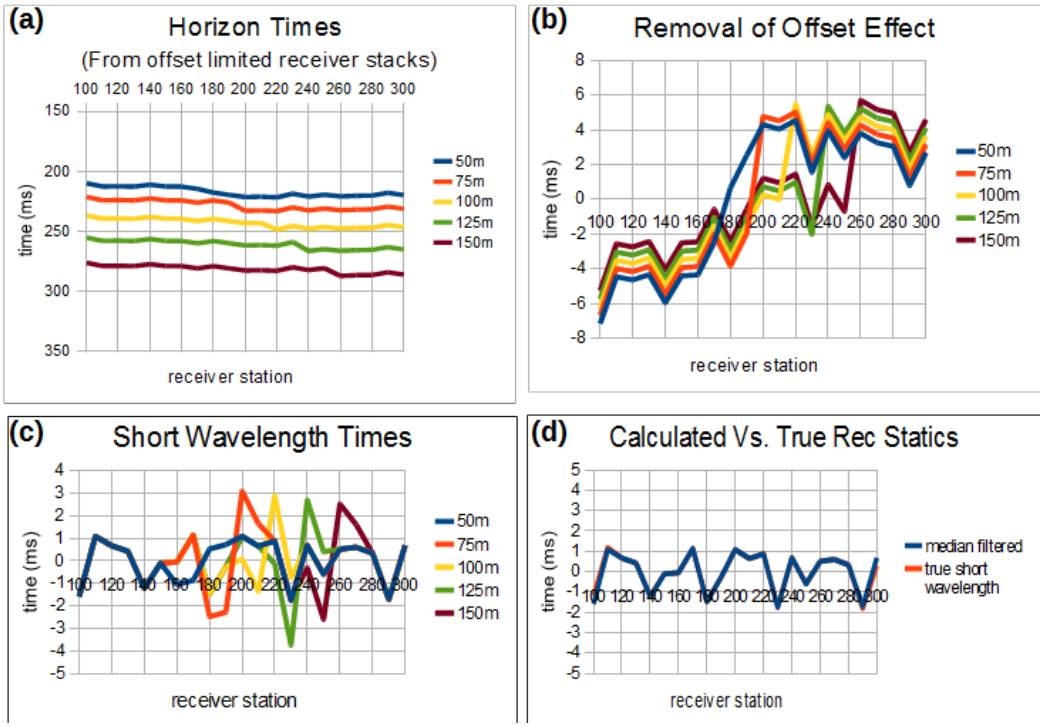

Figure 3: Synthetic demonstration of robust statistical statics calculation. This uses a simple surface-consistent numerical model based on equation 2 with a reflector at approximately 150m depth dipping to the left and includes a fault in the middle. (a) Horizon picks from limited-offset receiver stacks. These can be used in either the surface-consistent or robust statistical algorithms. (b) Following removal of offset terms. (c) Short-wavelength component. (d) Comparison of the true short-wavelength receiver static and the robust statistical solution.

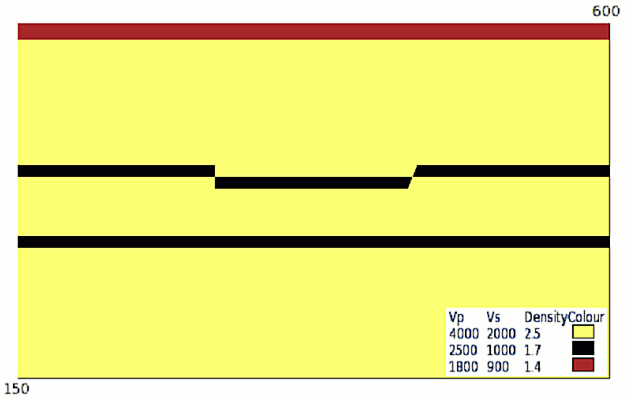

Figure 4: 2D Model used in the viscoelastic finite-difference investigation. Horizontal and vertical dimensions are 600m and 150m respectively. Includes two 5m thick coal seams, at depths of 60m and 90m

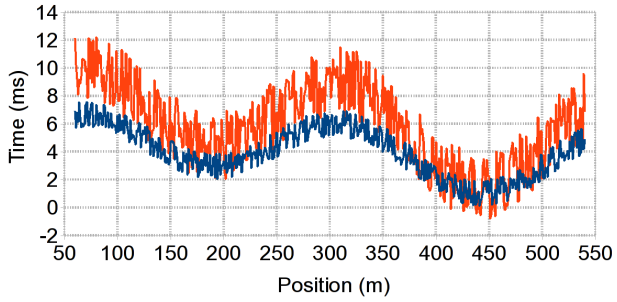

Figure 5: Synthetic near-surface statics for P (blue) and S waves (red), based on realistic short and long-wavelength variations.

too much noise on the near (ground roll) and far offsets (weak signal). Figure 7 shows the receiver statics for a representative section of the model. These have been calculated via the surface-consistent technique using the least-squares inversion algorithm. The corresponding true receiver statics solution is also given as a reference. This figure indicates that overall the surface-consistent approach provides a good estimate of the receiver statics, especially for the shorter wavelengths. However, at the lower numbered receivers the calculated statics diverge from the true statics. This is due to there being a low number of horizon picks associated with the receivers in this region. This causes the least-squares inversion to become unstable. In this case the reduced number of picks was intentional. This was done to demonstrate the influence of pick density. For a real dataset this could correspond to a region of high noise, reduced trace density (e.g. near the ends of lines), or high signal attenuation. This signal attenuation may in fact be caused by the weathering variations that we are trying to identify. Unfortunately the relationship is difficult to quantify, such that we can not exploit the effect in our algorithm. The practical impact of the attenuation is to degrade the statics solution.

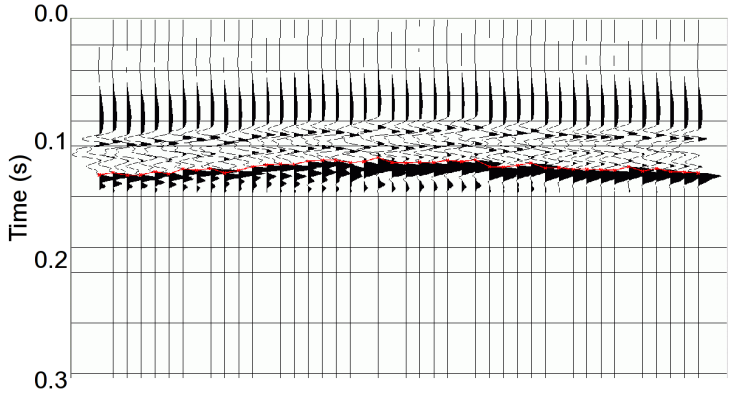

Figure 6: Offset-limited (250m) receiver stack. The first reflection horizon has been picked (red). The deeper reflectors and groundroll noise have been muted to emphasise the reflector.

Figure 8 shows the receiver statics solution generated via the robust statistical method. This has utilised the same horizon picks as for the surface-consistent technique. This demonstrates that the robust method can give a very good solution to the receiver statics. Note that it has also provided a good solution in the region where the surface-consistent inversion has become unstable. This suggests that the robust method may be useful for situations where there are limited horizon picks that can cause

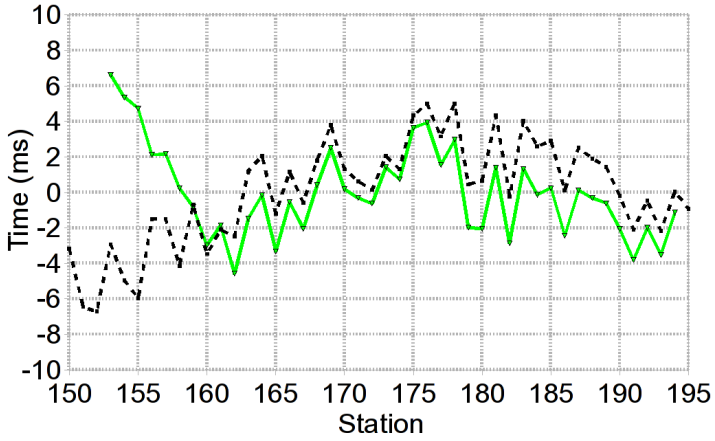

Figure 7: Comparison of the surface-consistent receiver-statics solution (green) and the true-solution (black) for a section of the model. Note that DC bias has been removed from each curve for easier comparison.

the surface-consistent approach to be less reliable. Note, however, that if the signal-to-noise ratio of the offset-limited stacks becomes too poor the robust method may also become less reliable.

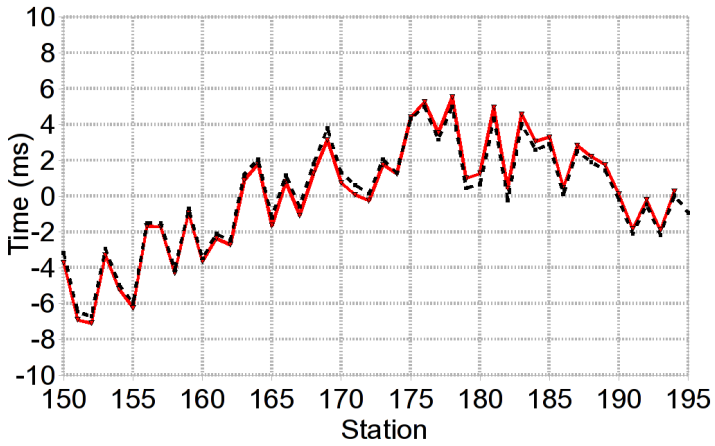

Figure 8: Comparison of the robust statistical receiver-statics solution (red) and the true-solution (black) for a section of the model.

The final approach used on the modelled data was the PPS refraction statics method. Figures 9a and 9b show the vertical and inline shot records for a representative location in the model. On Figure 9a, a red dashed line indicates the slope and general location of the PPP refraction event. This event is the first energy on the vertical record and is usually picked in

conventional P-wave processing to determine the statics solution. An analogous event for PS processing is the PPS refraction event (Figure 9b). The slope of the PPS event is the same as the PPP event, since both have the same wave type (P) along the refractor. The PPS refraction comes in later than PPP, and may not be the first energy on the record. As is apparent from Figure 9, the PPS event is generally weaker. These factors can make it difficult to pick PPS refractions on real seismic records.

Figure 10 shows the receiver statics solution for the PPS refraction statics calculated via the time-term technique. This suggests that provided the PPS refraction event can be picked, a very good receiver-statics solution can be obtained.

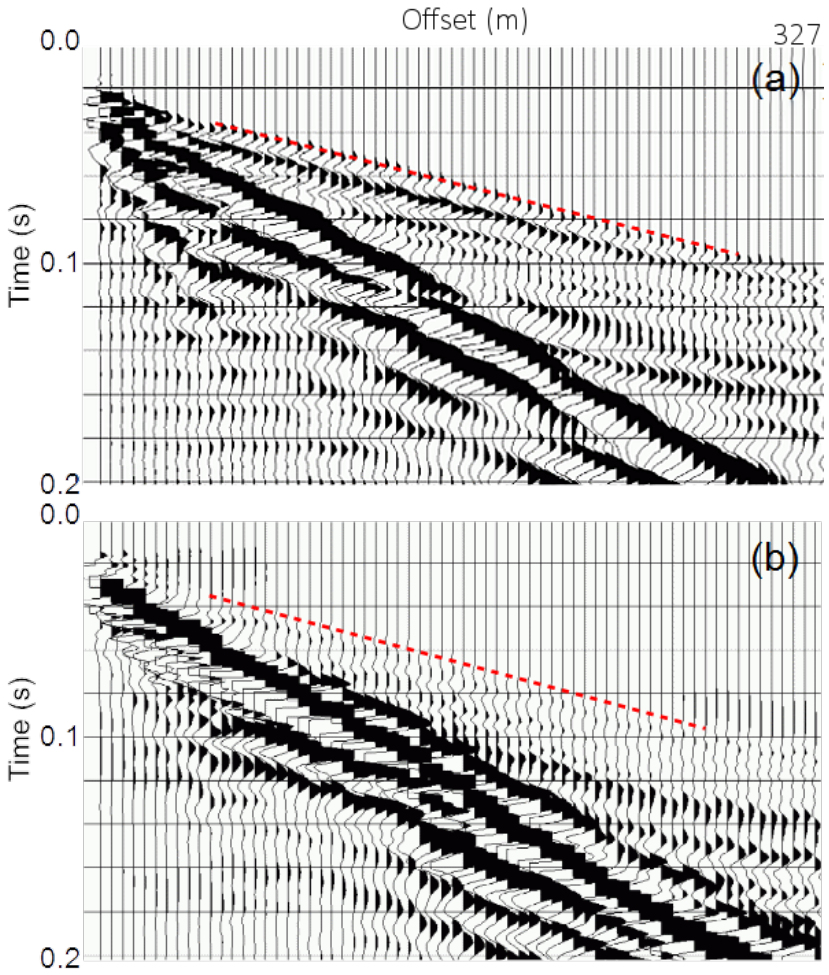

Figure 9: Example vertical (a) and inline (b) records from the modelled data. The red line on both images is a guide representing the expected PPP refraction time for a constant weathering depth. The PPP refractor is the first arrival on the vertical record (event in the vicinity of the red line). The PPS refractor is the weaker event on inline record that is lagging after the red line. In this case it is the inline first arrival due to the method of building the synthetic data. This is not necessarily the case for real datasets.

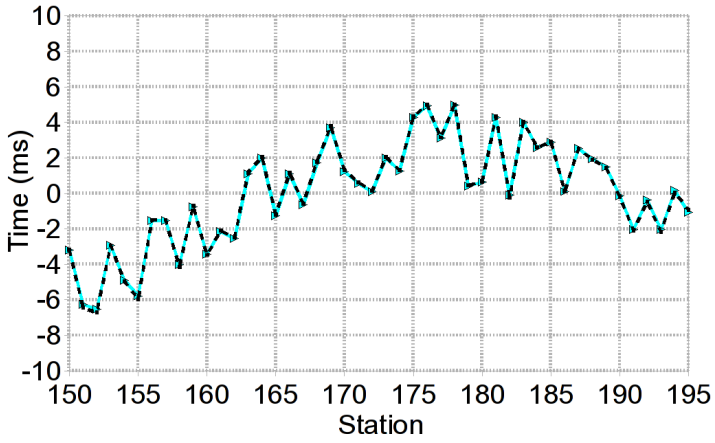

Figure 10: Comparison of the time-term PPS-refraction receiver-statics solution (cyan) and the true-solution (black) for a section of the model.

3D-3C TRIAL

This investigation into PS statics has been conducted as part of shallow 3D-3C trial examining the feasibility of acquiring and processing coal-scale PS-wave data in conjunction with conventional P-wave data (Strong & Hearn, 2011). The survey was acquired at a location within the Bowen Basin, NE Australia, using a Vibroseis (IVI Envirovibe) surface source. The grid covered 1200m x 500m, incorporating 10 receiver lines and 44 non-orthogonal source lines. Table 1 gives the basic survey parameters.

Table 1: Survey geometry

Receiver spacing	15m
Receiver line spacing	30m
Source spacing	30m (34.64m in source line direction)
Source line spacing	30m
Source line orientation	60° from receivers, staggered (±7.5m)

The terrain was generally flat to gently undulating with creek cuttings causing localised elevation variations of up to 3m (Figure 11a). The surface soil layers consisted of a brown clayish layer for most of the survey area. The southern third of the survey consisted of a black soil terrain (Figure 11b). This layer had many large cracks and tended to crumble when excavated for geophone burial. An examination of a cutting in the area suggested that the black soil overlays the brown soil layer having a thickness of 1-2m at the southern end and thinning toward the north. These surface conditions were expected to generate significant variations in the PS statics.

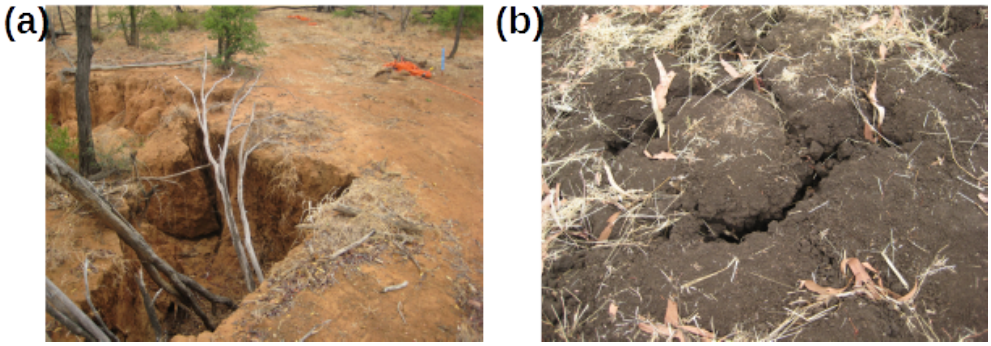

Figure 11: Surface conditions of the trial area consisted of a brown weathering layer in the north (a) and a broken-up black soil region in the south of the survey (b).

Figure 12 gives a simplified geological model that was expected for this survey based on earlier seismic and infield investigations.

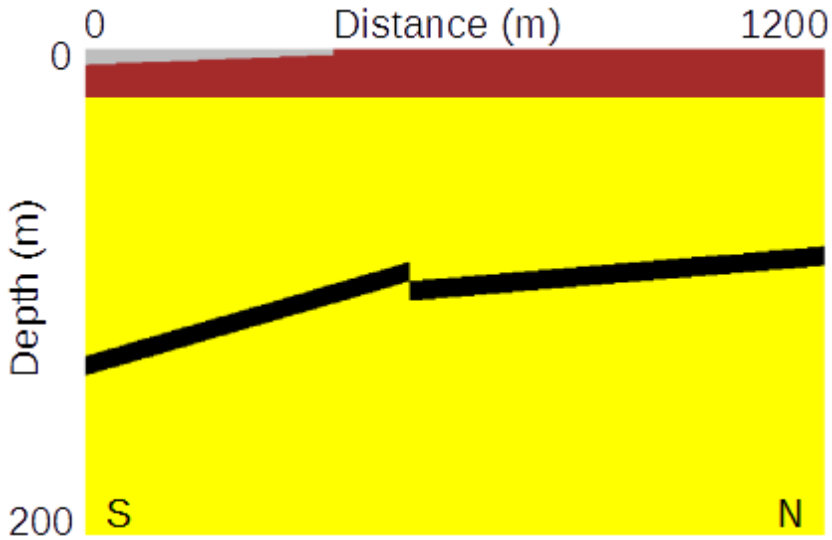

Figure 12: Expected geology based on an earlier 2D P-wave seismic line and a nearby borehole. The grey and red layers represent the possible weathering layers observed by surface investigations. The survey is dominated by a primary coal seam (black) dipping toward the south.

Results

The first receiver statics technique applied to the 3D dataset was the standard surface-consistent statics method. The source static corrections were calculated using conventional PPP refraction techniques and applied prior to estimation of S-wave receiver statics. The coal geology results in a single dominant reflector which was used for the horizon picks.

An important part of this trial was to examine the impact of azimuthal variations on PS data processing. Therefore, surface-consistent receiver statics were estimated for limited-azimuth datasets (20 degree increments). Figure 13 gives a representative example of the calculated receiver statics for two azimuthal directions, on two adjacent receiver lines. If results such as these were geologically real (rather than inversion artefacts), it would imply very significant azimuthal variation of the receiver statics.

However, we would not expect to observe such azimuthal variations. As discussed in connection with equation 6, PPS rays are typically close to

vertical in the vicinity of the receiver. Hence, rays from different azimuths will travel very similar paths. Based on this logic, the azimuthal variations exemplified in Figure 13 seem to be artefacts of the inversion.

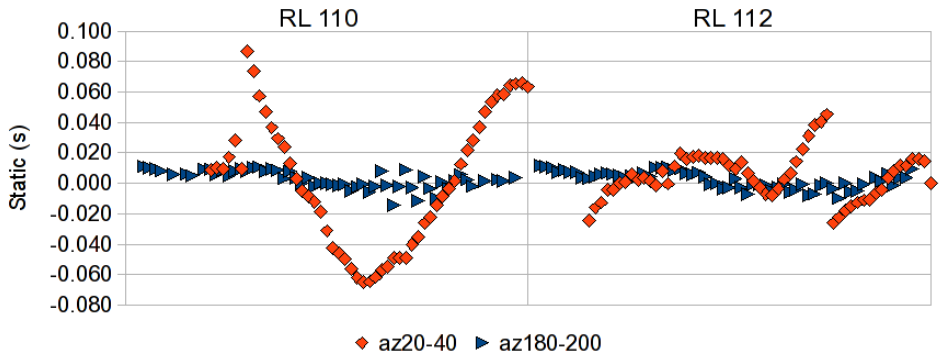

Figure 13: Representative limited-azimuth receiver-statics solutions obtained using the PS surface-consistent approach.

To further evaluate this statics method we have examined azimuths that give similar receiver-statics solutions (Figure 14a). If a receiver statics solution was derived using the horizon picks from all of these azimuths, we would expect the combined solution to have a similar trend to the average of the limited-azimuth solutions. However, as is demonstrated in Figure 14b the combined solution can, in some cases, be very different. Again, this is an example of non-uniqueness in the least-squares inversion. In this case it is caused by parameter leakage between the structure and receiver components, where some of the time delays associated with the structure of the reflection event are interpreted as receiver statics. This particular leakage is not unexpected in shallow PS reflection. Ray-path asymmetry means that the reflection point can be significantly displaced toward the receiver, causing the structural and receiver terms to have similar lateral coordinates. The inconsistency of the inversion results tends to be more pronounced in the southern half of the survey, in the vicinity of the black soil cover. This is possibly contributed to by weaker reflection signal (associated with near-surface scattering), larger statics variations, and reduced first-break pick density. For this dataset, the standard surface-consistent approach does not appear to be a reliable option for 3D PS statics estimation.

To determine the effectiveness of the other techniques we have used a reference processing flow where only the elevation statics have been applied to both sources and receivers. This approach corrects for lateral variations

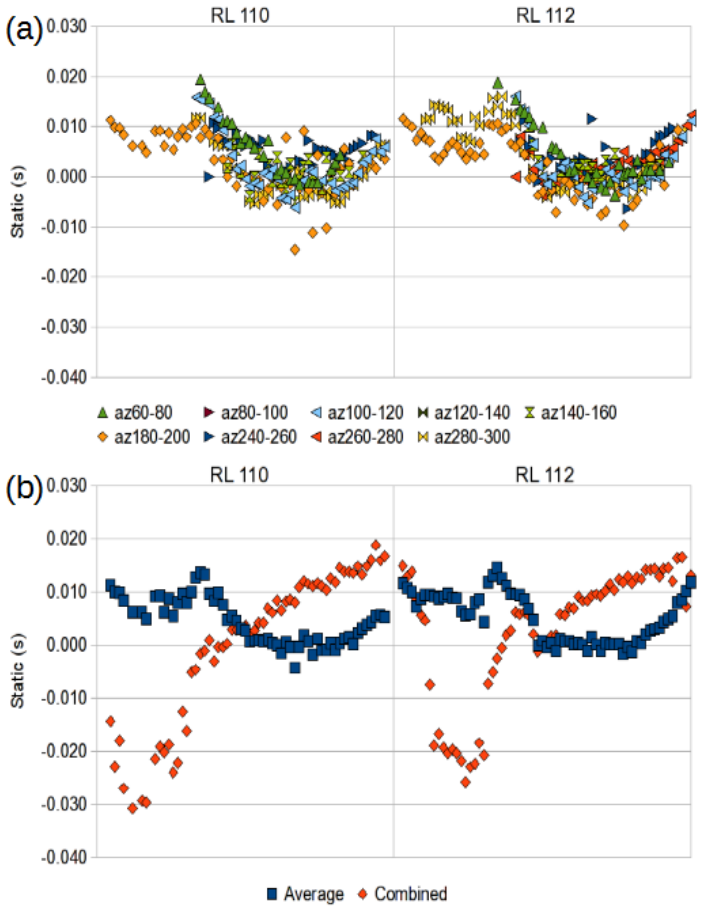

Figure 14: Evaluation of azimuthal variation in receiver-statics solutions. (a) limited-azimuth surface-consistent solutions displaying similar properties. (b) comparison of the average solution from the surface-consistent statics in (a) versus a solution incorporating all the input data from each of the curves in (a).

in surface elevation, but it assumes a constant weathering profile. The elevation-statics correction is easily implemented and can provide reasonable results if the weathering layer is simple with little variation. Figure 15 shows a representative stacked section (Line 112) extracted from the 3D volume. Figure 15b presents the reference section with only elevation statics applied.

Figure 15c shows the stacked section of Line 112 with robust statistical receiver-statics applied. This image has improved reflector continuity compared to the reference section (Figure 15b) especially toward the left end of the line, where the black-soil weathering layer might be expected to cause the elevation statics solution to be inaccurate. Note, however,that the structure on the robust section (Figure 15c) has a long-wavelength rolling nature that is not expected in the geology (Figures 12 and 15a). The inability of the robust method to correct for long-wavelength receiver-statics has been discussed above.

The final algorithm tested was the time-term PPS refraction approach. Figure 16 shows representative field records from the trial survey with the PPS refraction picks marked by red crosses. The quality of the PPS arrivals is variable, and picking of this event is more difficult than for PPP refractions. If the trace was too noisy the refraction was not picked or not included on the inversion. This particular 3D survey had very high fold, such that there are many traces contributing to each receiver location. Even when a large percentage of the refraction picks were not viable, we were still able to obtain a valid solution. This may not always be the case for production 2D or 3D-3C surveys.

Figure 15d shows the stacked section of receiver Line 112 with the PPS-refraction solution applied. This shows reasonable reflector continuity, although possibly not quite as good as the robust solution. The long-wavelength structural behaviour of the PPS stack is, however, more realistic than either the elevation or robust solutions, and is more in keeping with our expected geology (Figure 12).

A more in-depth comparison of the PPP and PPS refraction statics has been included in Figure 17. This compares the P-wave receiver statics from conventional PPP refraction (Figure 17a) to the S-wave receiver statics from PPS time-term refraction (Figure 17b). While the S-wave statics are larger than the P-wave statics, they broadly depict similar characteristics. These generally correspond to the elevation profile (Figure 17c) and suggest that the statics may be dominated by the weathering thickness. Note that there exist localised variations between the character of the P and S statics

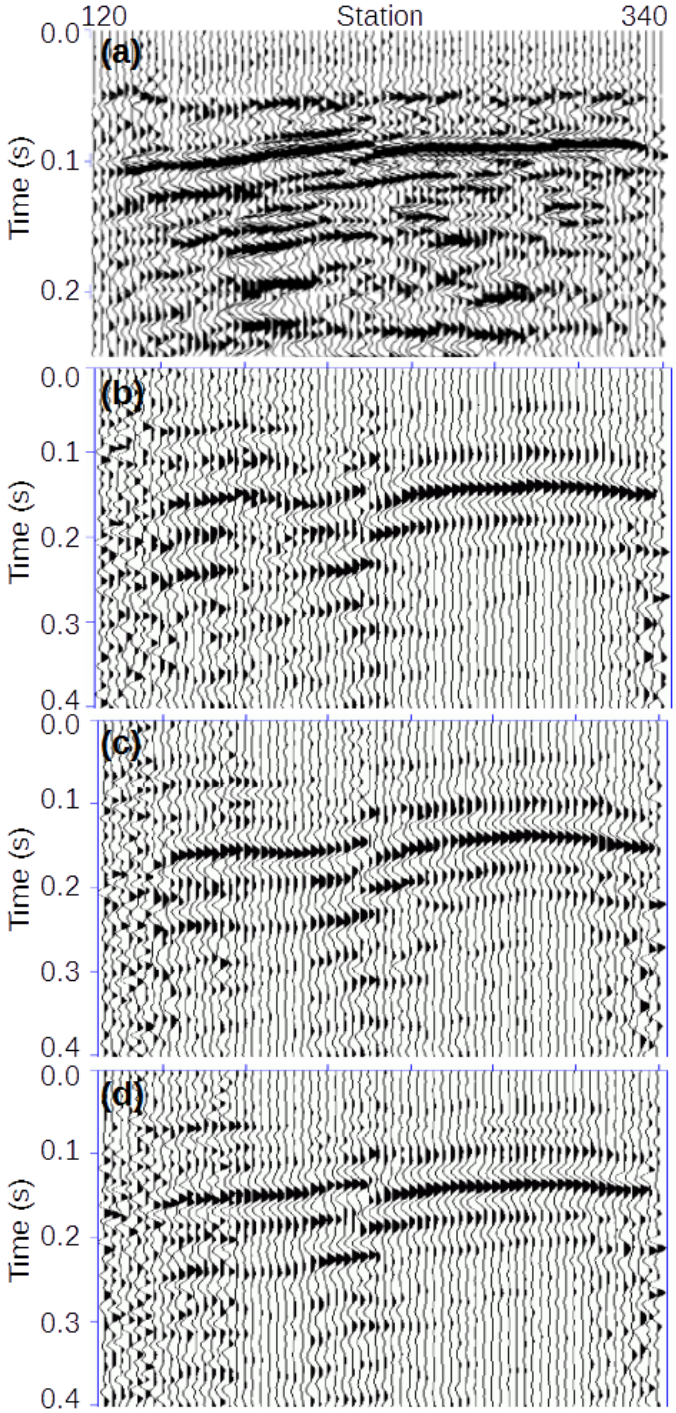

Figure 15: Representative reference section (Line 112) for receiver-statics comparison. (a) The P-wave CDP section is presented for structural comparison. (b)-(d) PS CCP stacked sections corresponding to the same location with varying statics corrections: (b) elevation-statics correction. (c) robust statistical receiver-statics correction. (d) time-term PPS refraction-statics correction.

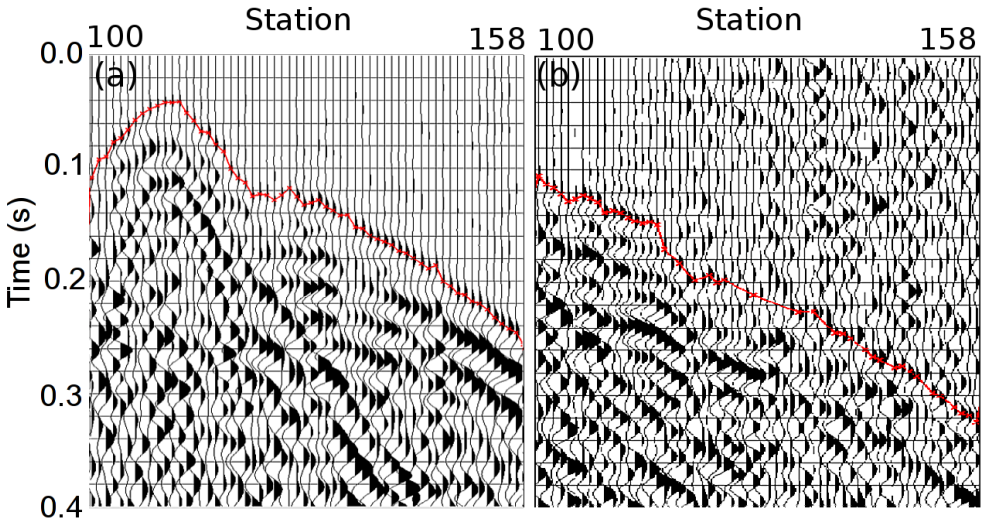

Figure 16: Comparison of representative receiver lines from sources at different sections of the 3D-3C survey. (a) Good quality record. (b) noisy record. The PPS refraction picks are indicated by the red crosses and a connecting red line. The refraction picks have been attempted for each record. However, there is much uncertainty in the location of PPS refraction on the noisy data. Most of these picks were omitted for the inversion.

particularly in the south (Inline stations 135-225). This supports the view that scaled P-wave receiver statics do not provide an optimal solution to the S-wave statics problem.

CONCLUSIONS

Shallow PS reflection imagery has theoretical potential to provide improved resolution, but this is dependent on maintaining good bandwidth in the CMP stack. In this context, statics correction is a critical, but challenging, component of shallow 2D and 3D PS reflection processing. Three approaches to this problem have been presented. The surface-consistent PS statics method is considered to be a useful standard. It is logistically convenient, but may produce incorrect solutions in environments where the signal-to-noise ratio is low, or when the reflector is shallow. These factors can result in instabilities in the inversion algorithm, and contamination of the receiver statics solution with noise or structural terms (parameter leakage). This is further influenced by errors and limitations at the horizon picking stage.

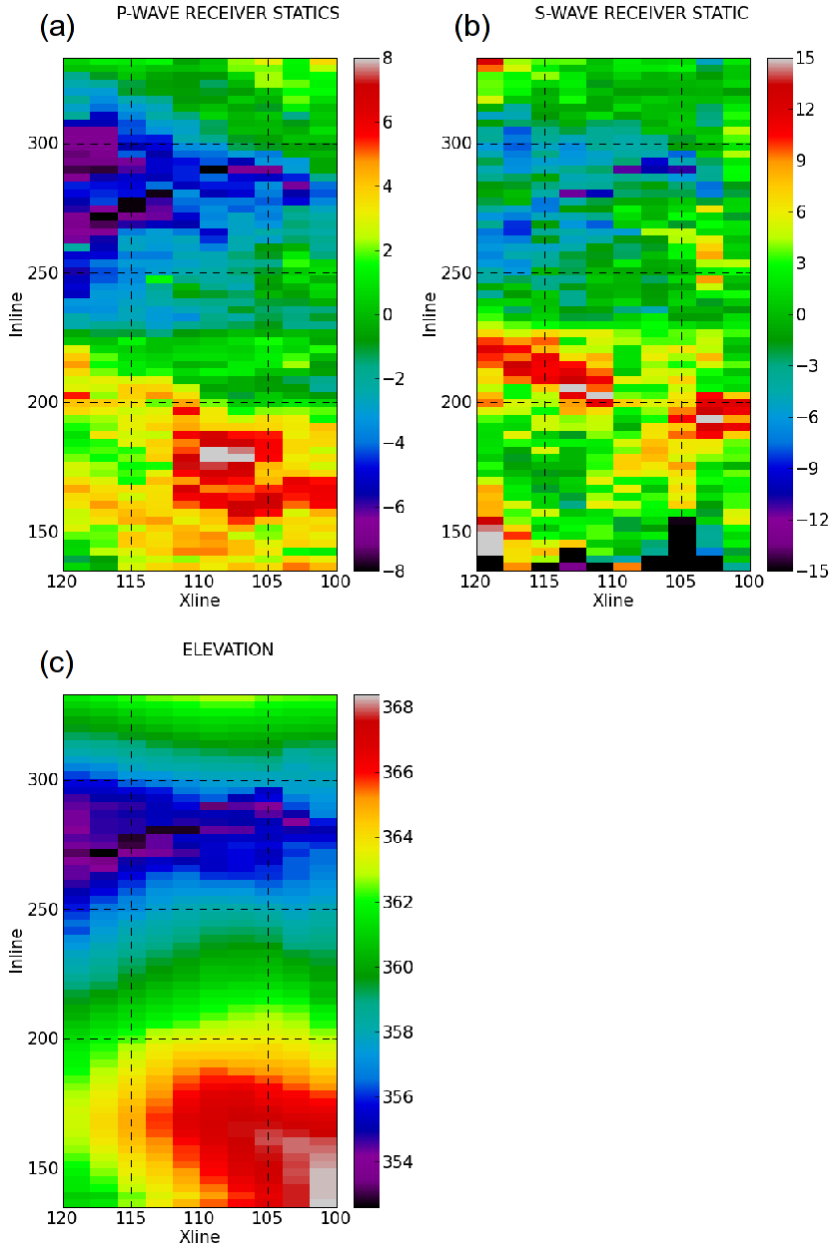

Figure 17: Map view of normalised receiver statics and elevations across the 3D survey area. (a) P-wave receiver statics generated by PPP refraction analysis of the vertical-component first breaks. (b) S-wave receiver statics generated using the inline data and the PPS time-term method. (c) Elevation. The elevations are given in meters and the statics in milliseconds. The S-wave statics have been clipped to +/-15ms to enhance general trends.

The robust statistics approach produces reasonable event continuity, but the lack of long-wavelength control can produce errors in structural interpretation. For our high-fold real dataset, the time-term PPS refraction statics method produced the best statics solution. It exhibited good reflector continuity and resolution over most of the survey. It also provided realistic long-wavelength structural character. The performance of the technique can be expected to be more variable on datasets with lower fold, or poor quality PPS arrivals.

It is expected that the relative performance of the algorithms may vary from case to case. As with P-wave statics, sequential application of different algorithms may provide a methodology for deriving both short and long-wavelength PS statics solutions.

ACKNOWLEDGMENTS

We would like to acknowledge the Australian Coal Association Research Program (ACARP) for support of this research.

REFERENCES

1. Brzostowski, M., Zhu, X., Altan, S., Thomsen, L., Barkved, O., Rosland, B. & Amoco, B. *3-D converted-wave processing over the Valhall field* in *1999 SEG Annual Meeting* (1999).
2. Cary, P. W. & Eaton, D. W. A simple method for resolving large converted-wave (P-SV) statics. *Geophysics* **58,** 429–433 (1993).
3. Cova, R., Henley, D. & Innanen, K. *Addressing Shear Wave Static Corrections in the Ray Parameter Domain: A Non-Stationary Interferometric Approach* in *2015 SEG Annual Meeting* (2015).
4. Guevara, S. E., Margrave, G. F. & Isaac, H. *A method for converted wave receiver statics correction in the CRG domain* in *2015 SEG Annual Meeting* (2015).
5. Hearn, S. Shallow, high-resolution converted-wave seismology for coal exploration. *ASEG Extended Abstracts* **2004,** 1–4 (2004).
6. Hearn, S. & Meulenbroek, A. Ray-path concepts for converted-wave seismic refraction. *Exploration Geophysics* **42,** 139–146 (2011).

7. Hearn, S., Hendrick, N. & McMonagle, J. Converted-wave seismic reflection for improved resolution of coal structures. *ACARP Report* **C10020** (2003).

8. Hendrick, N., Hearn, S. & Strong, S. Integrated P/PS seismic imaging for improved geological characterisation of coal environments. *ACARP Report* **C13029** (2007).

9. Henley, D. *Raypath interferometry vs. conventional statics: Recent field data and model comparisons* in *SEG Technical Program Expanded Abstracts 2014* (Society of Exploration Geophysicists, 2014), 2040–2044.

10. Lawton, D. C. Computation of refraction static corrections using first-break traveltime differences. *Geophysics* **54,** 1289–1296 (1989).

11. MacLeod, M., Hanson, R., Hadley, M., Reynolds, K., Lumley, D, McHugo, S & Probert, A. *The Alba Field OBC Seismic Survey* in *6th International Congress of the Brazilian Geophysical Society* (1999).

12. Meulenbroek, A. & Hearn, S. Analysis of converted refractions for shear statics and near-surface characterisation. *Exploration Geophysics* **42,** 147–154 (2011).

13. Ralston, M. *Estimation of Delay Time Refraction Statics by Regularized Inversion of First Arrival Times* in *2015 SEG Annual Meeting* (2015).

14. Reiter, L. An investigation into the time term method in refraction seismology. *Bulletin of the Seismological Society of America* **60,** 1–13 (1970).

15. Simin, V., Harrison, M. P. & Lorentz, G. A. Processing the Blackfoot 3C-3D seismic survey. *CREWES Research Report* **8(39)** (1996).

16. Socco, L. V., Mabyalaht, G. & Comina, C. *Robust static estimation from surface wave data* in *2015 SEG Annual Meeting* (2015).

17. Stewart, R. R., Gaiser, J. E., Brown, R. J. & Lawton, D. C. Converted-wave seismic exploration: Methods. *Geophysics* **67,** 1348–1363 (2002).

18. Strong, S. & Hearn, S. Multi-component seismic-resolution analysis using finite-difference acquisition modelling. *Exploration Geophysics* **39,** 189–197 (2008).

19. Strong, S. & Hearn, S. Towards 3D, integrated P+PS seismic imaging of coal targets. *ACARP Report* **C17029** (2011).

20. Thomsen, L. Converted-wave reflection seismology over inhomogeneous, anisotropic media. *Geophysics* **64,** 678–690 (1999).

21. Vargas, J., Monsegny, J., Agudelo, W. & Montes, L. *Comparative analysis of C-wave receiver static estimation in onshore data* in *12th International Congress of the Brazilian Geophysical Society* (2011).

22. Yang, C., Wang, Y. & Lu, J. Application of Rayleigh waves on PS-wave static corrections. *Journal of Geophysics and Engineering* **9,** 90 (2012).